This is an open access article published under an ACS AuthorChoice License, which permits copying and redistribution of the article or any adaptations for non-commercial purposes.

ACS OMEGA

Article

Cite This: ACS Omega 2019, 4, 22057−22068

http://pubs.acs.org/journal/acsodf

Amino Acid-Fabricated Glassy Carbon Electrode for Efficient Simultaneous Sensing of Zinc(II), Cadmium(II), Copper(II), and Mercury(II) Ions

Tayyaba Kokab,[†] Afzal Shah,[*,†,‡] Faiza Jan Iftikhar,[†,§] Jan Nisar,[∥] Mohammad Salim Akhter,[‡] and Sher Bahadur Khan[⊥]

[†]Department of Chemistry, Quaid-i-Azam University, Islamabad 45320, Pakistan

[‡]Department of Chemistry, College of Science, University of Bahrain, Sakhir 32038, Bahrain

[§]NUTECH School of Applied Sciences and Humanities, National University of Technology, Islamabad 44000, Pakistan

[∥]National Centre of Excellence in Physical Chemistry, University of Peshawar, Peshawar 25120, Pakistan

[⊥]Department of Chemistry, King Abdul Aziz University, Jeddah 21589, Kingdom of Saudi Arabia

ABSTRACT: Herein, we present a greener approach to achieve an ultrasensitive, selective, and viable sensor engineered by amino acids as a recognition layer for simultaneous electrochemical sensing of toxic heavy metals (HMs). Electrochemical techniques like electrochemical impedance spectroscopy (EIS), cyclic voltammetry (CV), and square-wave anodic stripping voltammetry (SWASV) were applied to demonstrate sensing capabilities of the designed analytical tool. The comparative results of different amino acids demonstrate alanine's superior performance with a well-resolved and enhanced current signal for target metal ions due to strong complexation of its functional moieties. The working conditions for alanine-modified GCE were optimized by investigating the effect of alanine concentration, different supporting electrolytes, pH values, accumulation potentials, and time. The limits of detection for Zn^{2+}, Cd^{2+}, Cu^{2+}, and Hg^{2+} were found to be 8.92, 5.77, 3.01, and 5.89 pM, respectively. The alanine-modified electrode revealed absolute discrimination ability, stability, and ultrasensitivity toward metal ions even in the presence of multifold interfering species. Likewise, greener modifier-designed electrodes possessed remarkable electrocatalytic activity, cost affordability, reproducibility, and applicability for picomolar level detection of HM ions in real water sample matrixes. Theoretical calculations for the HM−amino acid interaction also support a significantly improved mediator role of the alanine modifier that is consistent with the experimental findings.

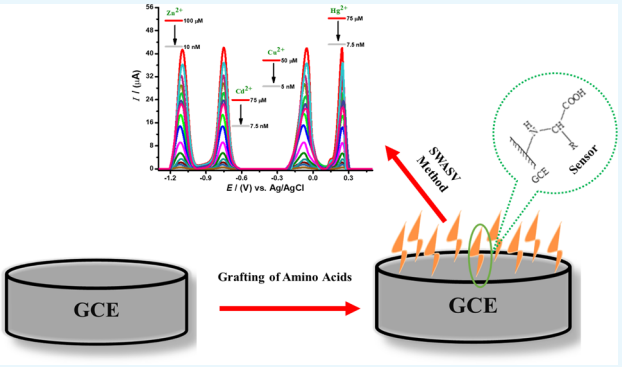

1. INTRODUCTION

Heavy metal (HM) ions (that have atomic density above 4−4.5 g/cm^3) are proclaimed by worldwide organizations like WHO, USEPA, and EPA as a risk to living species mainly due to their nonbiodegradable nature and tendency to bioaccumulate.[1] Major causes of heavy metal toxicity in living organisms have been attributed to urbanization and a concomitant exponential increase in human activities such as the indiscriminate use of pesticides and fertilizers, metal mining processes, automobile productions, bio solids and manures incineration, and liberation of industrial and municipal wastewater in drinking water bodies, which has irreversibly affected the natural environment.[2] Heavy metals can cause serious health hazards depending on the type of metal intoxication, its concentration and duration of exposure.[3] Although copper and zinc are considered as essential trace elements for human metabolism, yet, their excessive consumption can cause a number of complications, few being: major organ damage and failure, biocatalytic inhibition, DNA mutations, anemia, reduction in growth, and reproduction.[4−6] Cadmium has been declared as carcinogenic and is poisonous even in low amounts due to its ability to bioaccumulate by replacing calcium in the body and causes serious disorders and impairment to functioning of vital organs.[7,8] Similarly, mercury poisoning may lead to several fatal complications in the body.[9,10] Therefore, the detection and elimination of these HMs from water resources are ever more necessary for public health safety.

Detection of inorganic water toxins, that is, heavy metal ions via classical analytical techniques, involves tedious sample preparation, complex operations, expensive, and nonportable equipments as reported in literature.[11,12] Therefore, the development of a user-friendly, robust, selective, and highly sensitive green analytical platform for the simultaneous

Received: September 28, 2019
Accepted: November 22, 2019
Published: December 9, 2019

© 2019 American Chemical Society

DOI: 10.1021/acsomega.9b03189
ACS Omega 2019, 4, 22057−22068

detection of HMs is of utmost importance. In this regard, electrochemical analytical methods offer an easy, onsite, and adaptable approach for trace level detection of HMs. Amongst these methods, anodic stripping voltammetry (ASV) is the method of choice over conventional methods as it is of low cost and offers short analytical time, a wide electrochemical window, and a favorable signal-to-noise ratio that allows trace level detection of species.[8,12] Additionally, modification of the working electrode with an electroactive recognition layer in ASV promises improved functionality of the sensor with enhanced oxidation signals, detection limits, and selectivity for the respective metal ions.

Recognition layers constituting various molecules including organic, inorganic, bio-, nanomaterials, and surfactants have been widely reported as electrochemical sensors for metal ions.[8,10,13−19] Similarly, amino acids and peptides are reported to be used as a recognition layer on the electrode surface for metal ion detection whereby strong complexes with metal ions are formed, and hence, an effective sensing probe is developed.[20−22] Electrochemical sensors based on amino acids have a number of advantages over other modifiers that include their tendency to bind with metal ions through their chelating moieties such as amino $-NH_2$, carboxylic $-COOH$, hydroxyl $-OH$, or thiol $-SH$ groups having charge donating and complex stabilizing abilities, favorable adsorption sites, eco-friendliness, availability in nature, and hence being economical.

In this perspective, the present research describes the design and fabrication of an amino acid-based ultrasensitive electrochemical sensor for detecting toxic metal ion concentrations below the threshold value suggested by EPA and WHO. To this end, four different amino acids, alanine, threonine, lysine, and glutamic acid, that is, a nonpolar, a polar, a basic, and an acidic amino acid, respectively, have been used to develop an electrochemical sensor for simultaneous detection of zinc, cadmium, copper, and mercuric (Zn^{2+}, Cd^{2+}, Cu^{2+}, Hg^{2+}, respectively) ions in spiked and real samples. In present work, amongst the different modifiers, best sensing properties were observed by using alanine as the recognition layer due to its highly favorable interactions with the targeted metal ions. We believe that this is the first work of its kind reporting a simple, cost affordable, and easy to use electrochemical method based on an amino acid-modified electrode for sequestering toxic HM ions such as Zn^{2+}, Cd^{2+}, Cu^{2+}, and Hg^{2+} down to picolevel concentrations in water systems with robust and novel figures of merit.

2. RESULTS AND DISCUSSION

2.1. Electrochemical Characterization of the Amino Acid-Fabricated Electrode. Cyclic voltammetry (CV) was performed to characterize amino acid-modified electrodes by probing a current response of the 5 mM $[Fe(CN)]^{3-/4-}$ redox couple in contrast to bare GCE in 0.1 M KCl as the supporting electrolyte. Figure 1A demonstrates a noticeable increase in the reversible electrochemical signal of the $[Fe(CN)]^{3-/4-}$ redox couple at amino acid-immobilized GCE compared to bare GCE, indicating that amino acids facilitate accessibility of the redox probe to the electrode surface by reducing the barrier to interfacial electron transfer processes and enhancing the current signals. However, the most intense signals were achieved with alanine-modified GCE due to its small size and simple molecular geometry that allows more alanine molecules to occupy the electrode surface. Consequently, the

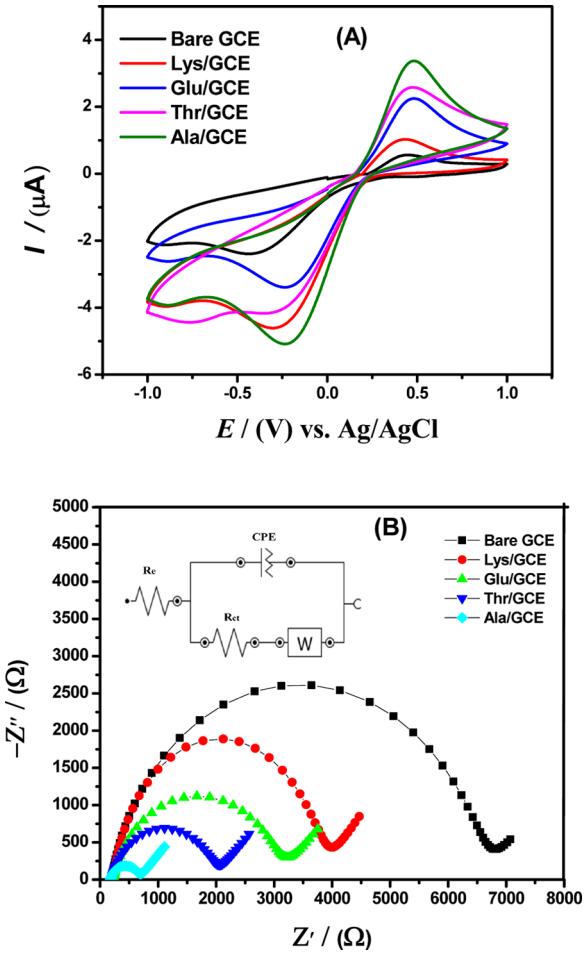

Figure 1. Comparative (A) cyclic voltammograms obtained from bare GCE and alanine, threonine, glutamic acid, and lysine amino acid-modified GCE in a medium containing 5 mM $K_3[Fe(CN)_6]$ solution and a 0.1 M KCl electrolyte. (B) Nyquist plots using electrochemical impedance spectroscopic data with applied frequency ranges varying from 100 kHz to 0.1 Hz. (Inset) Randles equivalent circuit model for the system under study showing resistors, capacitor, and Warburg impedance elements.

presence of more alanine molecules at the electrode surface not only creates more active sites for analyte accumulation but also provides faster electron transduction of the redox probe at the interface of the designed sensor.

Successful fabrication of the modified working electrode and charge transduction of the redox probe via bare GCE and amino acid-modified GCEs were characterized by employing electrochemical impedance spectroscopy (EIS) in the form of Nyquist plots at a frequency ranging from 100 kHz to 0.1 Hz in an electrochemical cell employing a 5 mM aqueous solution of the $[Fe(CN)]^{3-/4-}$ redox couple in a supporting electrolyte of 0.1 M KCl. A semicircle portion of Nyquist plots shown in Figure 1B demonstrates the electronic transmission capability of the modified and bare electrodes with relation to the redox couple. A higher frequency range part of the Nyquist plot characterizes the charge-transfer controlled process, whereas a lower frequency range, that is, the linear section of the plot, demonstrates the dominance of the diffusional process.[23] Out of all modifiers, the smallest semicircular diameter obtained for Ala/GCE reflects enhanced interfacial electronic transduction of the redox couple toward the modified electrode and shows

DOI: 10.1021/acsomega.9b03189
ACS Omega 2019, 4, 22057−22068

Table 1. Randles Circuit Parameters Calculated for Bare and Amino Acid-Modified GCEs from Electrochemical Impedance Spectroscopy (EIS)

electrodes	R_{ct} (kΩ)	R_e (Ω)	CPE (μF)	J_o (μA/cm^2)	n
bare GCE	6.41 ± 0.057	201.7 ± 1.74	5.52 ± 0.54	4.01	0.79
Lys/GCE	3.34 ± 0.026	199.5 ± 1.68	2.57 ± 0.12	7.69	0.81
Glu/GCE	2.62 ± 0.025	198.2 ± 1.58	2.53 ± 0.10	9.80	0.83
Thr/GCE	1.77 ± 0.017	186 ± 1.41	2.51 ± 0.14	14.50	0.86
Ala/GCE	0.50 ± 0.007	179.8 ± 1.63	1.43 ± 0.04	51.40	0.90

reduced charge-transfer resistance (R_{ct}) as determined qualitatively. Thus, the alanine-modified electrode offers minimum resistance during interfacial charge transfer and provides excellent conductivity as compared to other amino acid-modified electrodes. Quantitative values of R_{ct}, n (quality factor of a capacitor), and constant phase element (CPE) enlisted in Table 1 were obtained from synchronization of EIS data with the Randles equivalent electric circuit model. The resistive values corresponding to Lys/GCE (R_{ct} = 3.34 kΩ), Glu/GCE (R_{ct} = 2.62 kΩ), Thr/GCE (R_{ct} = 1.77 kΩ), and Ala/GCE (R_{ct} = 0.50 kΩ) were lower than the bare GCE (R_{ct} = 6.41 kΩ), which indicates superior conductance and rapid heterogeneous electron transfer kinetics of the amino acid-based GCE especially for alanine-designed sensor, which corroborates well with the CV results, indicating successful fabrication of the electrode surface for achieving a more sensitive electrochemical sensing platform.

The remarkable electrocatalytic function of the modifiers at the electrode surface can be determined by a kinetic parameter, that is, an exchange current density (J_o), the value of which corresponds to the feasibility of electrochemical reaction at the electrode interfacial surface. The exchange current density (J_o) can be calculated by the equation $J_o = {}^{RT}/_{nFR_{ct}}$ where R, n, F, T, and R_{ct} are the gas constant, number of electrons involved in the electrode reaction (here n = 1 for $[Fe(CN)]^{3-/4-}$ redox reaction), Faraday's constant, temperature (here T = 298 K), and charge-transfer constant, respectively.[24] The higher exchange current density of alanine-modified GCE is attributed to an active electrode surface area due to availability of more alanine active sites which in turn offers less hindrance to the electron transfer of the redox probe as compared to other amino acids and bare GCE as listed in Table 1.

Square-wave voltammograms in Britton-Robinson buffer (BRB of pH 4) as a supporting electrolyte were recorded at bare and modified GCEs, functionalized with different amino acids viz alanine, threonine, glutamic acid, and lysine and demonstrated an enhanced oxidation current response in comparison to bare GCE for the detection of 10 μM Zn^{2+}, 7.5 μM Cd^{2+}, 5 μM Cu^{2+} and 7.5 μM Hg^{2+} ions. SWASV involves electroreduction at a deposition potential of −1.3 V for 140 s followed by their stripping from the modified electrode surface into solution during anodic stripping by scanning from −1.3 to 0.8 V. Similarly, electroreduction and stripping steps were applied on bare GCE for comparative voltammetric studies of respective metal ions with amino acid (AA)-modified electrodes. All modifiers exhibited an increase in the response of oxidation signals for Zn^{2+}, Cd^{2+}, Cu^{2+}, and Hg^{2+} ions than the bare GCE, which agrees with CV and EIS results as depicted in Figure 2. It is contended that electrodeposition of amino acids on GCE binds the amino group covalently with the GCE while the negatively charged carboxylic groups are freely available to uptake positively charged analytes.[25] The higher surface area of amino acid-modified GCEs under optimized conditions of

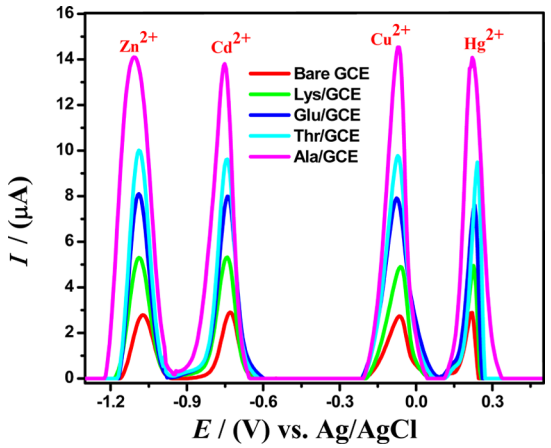

Figure 2. SWASV obtained from unmodified and alanine, threonine, glutamic acid, and lysine amino acid-modified GC electrodes for the detection of 10 μM Zn^{2+}, 7.5 μM Cd^{2+}, 5 μM Cu^{2+}, and 7.5 μM Hg^{2+} in BRB of pH = 4 as striping solvent, keeping a scan rate of 100 mV/s, a deposition potential of −1.3 V, and a deposition time of 140 s.

SWASV allows greater amounts of metal ions to be coupled to the surface, thus allowing it to accumulate more of the analytes than bare GCE. SWASV results revealed enhancement in the oxidation current I_p of the copper, cadmium, zinc, and mercury ions at the alanine-modified glassy carbon electrode owing to a provision of more adsorptive sites, which points toward easy accessibility of its carboxylic acid groups to metal ions in the solution for strong interactions between them. Another important factor to consider with regard to effective adsorption of amino acid at the electrode surface and its interaction with the analyte of interest is the steric hindrance as a result of its chemical structure. Hence, although threonine amino acid is polar in structure and has more electron donor functional groups, yet, its sensing behavior is inferior to alanine due to the steric hindrance of its comparatively bulky structure. Hence, alanine provides most intense SWV oxidative current signals I_p for given metal cations than the other investigated amino acids due to its small size, minimum steric hindrance, and simple molecular geometry, which affords faster electron transduction from analytes toward the electrode surface. Hence, for further electrochemical measurements, alanine amino acid was selected as the best electrocatalyst for simultaneous sensing of metals, Zn^{2+}, Cd^{2+}, Cu^{2+}, and Hg^{2+} ions.

2.2. Optimization of Conditions for the Best Performance of Alanine Modifier. The experimental conditions that affect the intensity and shape of peaks were investigated to get the maximum current signals by effective coordination of L-alanine with Zn^{2+}, Cd^{2+}, Cu^{2+}, and Hg^{2+} ions. The influences of various critical factors including concentration of the modifier, stripping electrolyte, pH of solution,[26] deposition potential, and accumulation time for preconcentration of metal ions were

DOI: 10.1021/acsomega.9b03189
ACS Omega 2019, 4, 22057−22068

studied at 100 μM Zn^{2+}, 75 μM Cd^{2+}, 50 μM Cu^{2+}, and 75 μM Hg^{2+} ions, and values were optimized for further investigations.

The increase in the alanine concentration on the GCE surface was found to significantly improve the magnitude of electro-oxidation signals for metals ions at the modified electrode that can be related to the provision of more active sites as the concentration of the modifier is increased. As the concentration of alanine increased, facilitation in the electron transfer process increased at the electrode surface up to an optimum concentration. However, after the optimum concentration of alanine, that is, 65 μM, a reduction in the peak current was noticed as evident from Figure 3A,B that can be

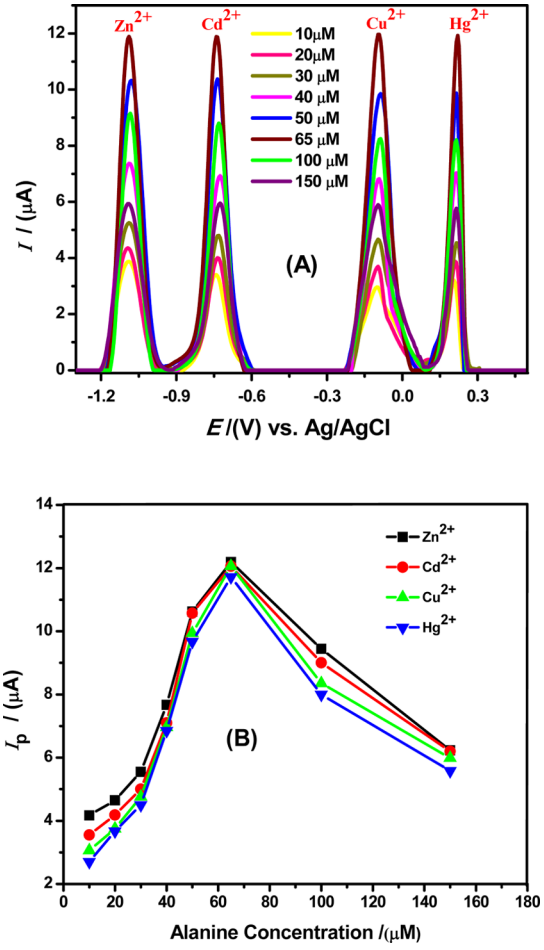

Figure 3. (A) Alanine concentration effect on the SWASV response of 100 μM Zn^{2+}, 75 μM Cd^{2+}, 50 μM Cu^{2+}, and 75 μM Hg^{2+} ions in BRB of pH = 4, keeping scan rate = 100 mV/s, deposition time = 5 s, deposition potential = −1.3 V by electrochemical assisted modification of GC electrode surface with different concentrations of alanine solution. (B) Plot of I_p vs alanine (modifier) concentration.

related to saturation of active sites, an increase in electrode resistivity and passive electron transfer due to multilayer adsorption of amino acid molecules over the electrode surface.

The SWASV responses of Ala/GCE for different metal ions in different electrolytic media were monitored in 0.1 M NaOH, 0.1 M H_2SO_4, 0.1 M HCl, 0.1 M KCl, phosphate buffer solution (PBS of pH = 7), Britton-Robinson Buffer (BRB of pH = 4), and acetate buffer solution (ABS of pH = 4.8) as supporting electrolytes. The supporting electrolyte helps to decrease the ohmic or $I-R$ drop and opposes the effect of migration current. The bar graph for quantification of the peak current intensity in the presence of various supporting electrolytes is illustrated in Figure 4A registered BR buffer of

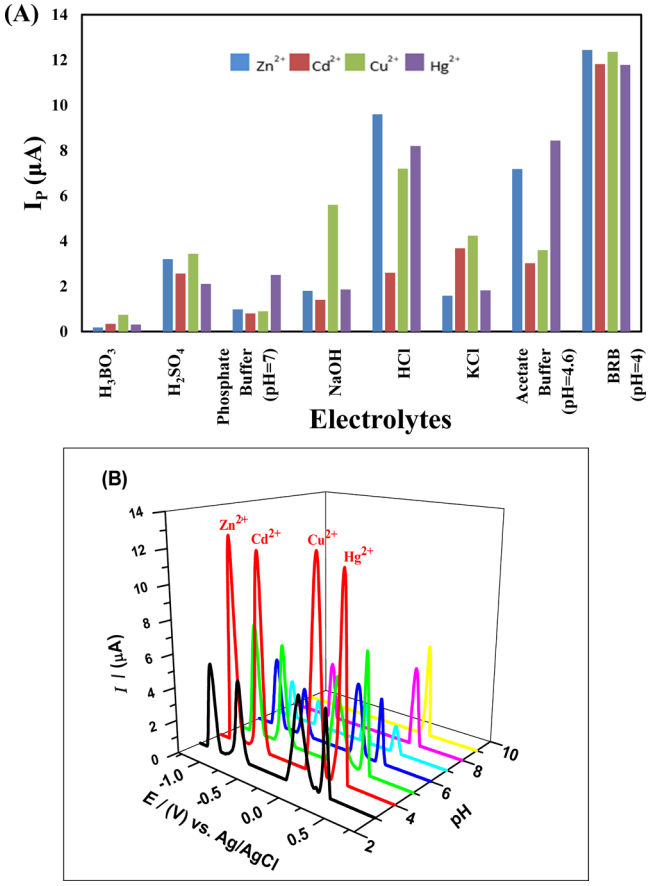

Figure 4. (A) Effect of various stripping media (supporting electrolytes) such as BRB (pH = 4), phosphate buffer (pH = 7), acetate buffer (pH = 4.8), 0.1 M HCl, 0.1 M NaOH, 0.1 M KCl, 0.1 M H_2SO_4, and 0.1 M H_3BO_3 on the SWASV peak currents of 100 μM Zn^{2+}, 75 μM Cd^{2+}, 50 μM Cu^{2+}, and 75 μM Hg^{2+} ions using 65 μM Ala/GCE, a deposition potential of −1.3 V, and an accumulation time of 5 s at a scan rate of 100 mV/s. (B) The plots of SWASV anodic peak currents I_p as a function of pH of BRB (3−9) obtained from 65 μM Ala/GCE at an accumulation time of 5 s, a deposition potential of −1.3 V with a scan rate of 100 mV/s.

pH 4 as the most suitable supporting electrolyte for stripping of electro-reduced metal ions back into the solution to provide well-resolved oxidation peaks for metal ions.

Similarly, pH of the supporting electrolyte influences the binding ability of the metal ions by having an impact on the electrode surface charge transduction,[26] proton availability in solution, and ionization of modifier functional groups. In this regard, the plots of E and I_p versus pH for 100 μM Zn^{2+}, 75 μM Cd^{2+}, 50 μM Cu^{2+}, and 75 μM Hg^{2+} ions as illustrated in Figure 4B were established by inspecting BRB in a wide range of pH values from 3.0 to 9.0 at a deposition time of 5 s to study the electrode reaction at an optimized pH value. The plot designates the maximum voltammetric signals at pH 4 of BRB that can be related to a pH-dependent ionization of the carboxylate group present in the chemical structure of alanine for effective complex formation with metal ions. However, at very low pH protonation of carboxylate ion results, thus having a low ability to complex with the metal ions, leading to a

DOI: 10.1021/acsomega.9b03189
ACS Omega 2019, 4, 22057−22068

decrease in oxidation signals for the metal ions. Similarly, at higher pH, formation of metal hydroxides is suggested, that is, $Zn(OH)_2$, $Cu(OH)_2$, $Hg(OH)_2$, and $Cd(OH)_2$, leading to decreased accessibility of the metal ions for electroreduction at the alanine-modified GCE.[27] Henceforth, BRB of pH 4 is selected as the optimum pH value to ensure a superior metal ion complexation ability of alanine for all the succeeding electroanalytical measurements.

The deposition step is quite critical to control preconcentrated accumulation of electrochemical species on the working electrode surface.[28] The dependence of redox behavior of selected analytes on the deposition potential at Ala/GCE was probed by varying the accumulation potentials from −0.9 to −1.5 V. Figure 5A reveals that increasing the negative deposition potential up to −1.3 V results in enhanced voltammetric signals, which can be attributed to the maximum accumulation of the metal ion species. Therefore, −1.3 V corresponds to the maximum coverage of the electrode surface with completely reduced analyte ions. Hence, the maximum loading of metals was accomplished at an accumulation potential of −1.3 V. Furthermore, the impact of the accumulation time on metal ion accumulation was also carried out by studying the increase in stripping peak currents with the preconcentration time. It was observed that the peak current increased with the deposition time up to 140 s at a deposition potential of −1.3 V as depicted in Figure 5B-I,II. However, when the deposition time exceeded 140 s, the amount of metals that can be reduced on Ala/GCE reached a limiting value as observed by a decrease in the value of current with time. This can be attributed to the complete surface coverage and saturation of available active sites of the working electrode with electro-reduced metals.[29] Therefore, as the deposition time increases, the thickness of the electro-deposited analyte layers at the modified electrode also increases and hinders any further mass transfer of metal ions.[30,31] Thus, 140 s was chosen to be the optimal preconcentration deposition time for the detection of corresponding Zn^{2+}, Cd^{2+}, Cu^{2+}, and Hg^{2+}ions. We can obtain the best SWASV response from Ala/GCE for simultaneous detection of Zn^{2+}, Cd^{2+}, Cu^{2+}, and Hg^{2+}ions by modifying GCE with 65 μM alanine solution in an analyte solution of BRB of pH 4, at a deposition potential of −1.3 V, and an accumulation time of 140 s.

2.3. Validation of Electrode Selectivity, Sensitivity, Stability, and Quantification of Limits. The limit of detection (LOD) and quantification (LOQ) of the sensor for a particular analyte can be assessed from expressions such as: LOD = $3\sigma/m$ and LOQ = $10\sigma/m$, where σ represents the standard deviation of n times replicate of voltammograms of the modified electrode in blank solution (electrolyte solution in the absence of analyte), and m is the slope of the concentration versus current plot.[32] Figure 6A depicts SWASV peaks obtained for simultaneous multiple metal ions in the concentration range from 100 μM down to 5 nM. It is observed in Figure 6A that, at high concentrations, the oxidative peak current shows nonlinearity. However, our developed electroanalytical sensor illustrates a board linearity range from 10 μM to 5 nM and the strongest correlation of the data, which is evidenced from the values of the correlation coefficient (R^2 = 0.99). Linear calibration curves of the alanine-modified electrode ranging from 5 to 100 nM shown in Figure 6B provide excellent LOD values, that is, 8.92, 5.77, 3.01, and 5.89 pM for zinc, cadmium, copper, and mercuric ions, respectively, which are far below the WHO and EPA

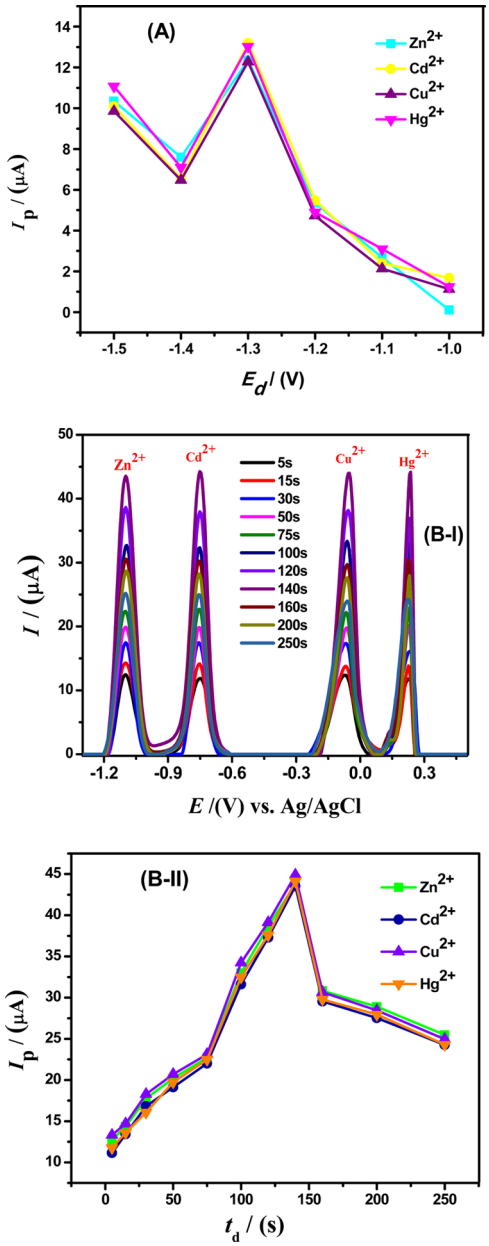

Figure 5. (A) Plot of I_p vs E_d shows the influence of accumulation potentials on the oxidative peak currents of 100 μM Zn^{2+}, 75 μM Cd^{2+}, 50 μM Cu^{2+}, and 75 μM Hg^{2+} ions in BRB of pH = 4, a scan rate of 100 mV/s, and a deposition time of 5 s at 65 μM Ala/GCE. (B-I) Effect of deposition times on the stripping current responses of 100 μM Zn^{2+}, 75 μM Cd^{2+}, 50 μM Cu^{2+}, and 75 μM Hg^{2+} ions in BRB of pH = 4 with a deposition potential of −1.3 V, and a scan rate of 100 mV/s at 65 μM Ala/GCE. (B-II) Plot between I_p vs t_d at different deposition times in BRB of pH = 4

recommendations.[1] Additionally, the Ala/GCE sensor offers low LODs for the metal cations under study as compared to other amino acid-based GCEs in this study. It was observed that an LOD of 3.01 pM for copper ions at Ala/GCE under optimized conditions was the lowest among any other metal cation detected. Similarly, cadmium and mercury with comparatively higher LODs of 5.77 and 5.89 pM at Ala/GCE showed almost equal current response and sensitivity of the modified electrode, while zinc still needed a higher concentration of 8.92 pM to be detected on Ala/GCE as compared to other metal cations. Hence, it is concluded that

DOI: 10.1021/acsomega.9b03189
ACS Omega 2019, 4, 22057−22068

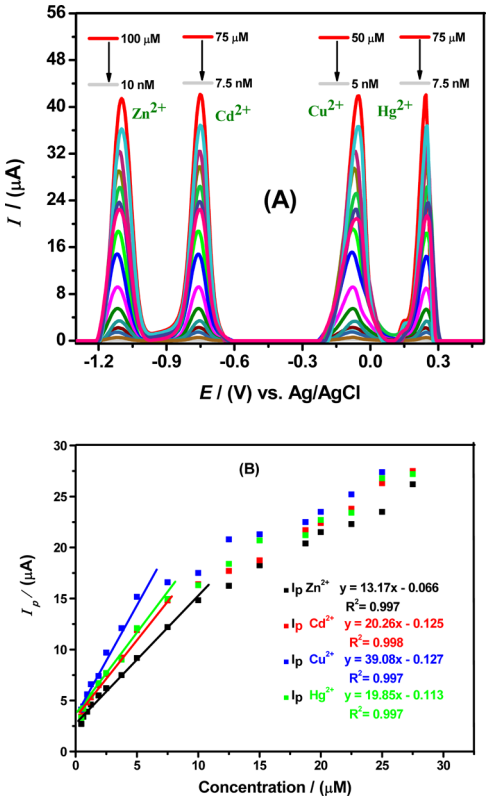

Figure 6. (A) SWASV recorded at Ala/GCE by varying concentrations of Zn^{2+}, Cd^{2+}, Cu^{2+}, and Hg^{2+} ions in BRB (pH = 4), a scan rate of 100 mV/s, a deposition potential of −1.3 V, and a deposition time of 140 s. The investigated concentration ranges are mentioned above each peak. (B) Corresponding calibration plots with linear equation and correlation values from data obtained from selected portion of plot-A SWASV showing linearity of Zn^{2+}, Cd^{2+}, Cu^{2+}, and Hg^{2+} ion concentrations with I_p obtained under chosen optimized conditions for Ala/GCE for each metal ions

alanine is most selective and sensitive for complexation with copper than other target analytes, but at the same time, it possesses better sensing ability and offers effective interactions for all metal cations under investigation than other amino acids as supported by theoretical calculations also(Section 2.5). Table 2 gives a comparison of analytical parameters such as LODs obtained from Ala/GCE for detection of metal ions compared to other electroanalytical metal sensors in literature. The table reveals promising sensitivity of our alanine-based sensor than graphene, carbon nanotubes, silver, gold, and cadmium tellurium nanoparticles, nanocomposites, organic ligands, and polymers fabricated sensors, which means that our developed amino acid sensor can detect trace level concentrations of metal ions more effectively.[9,10,26,32−50]

The designed sensor ability to discriminate the voltammetric response of respective metal ions in the presence of multifold concentrations of interfering agents like commonly occurring cations and anions in water and some strong complexing agents was thoroughly probed by electrochemical techniques, and their effect on the electro-oxidation signals of metal analytes is displayed in Figure 7A.[51] SWASV results reveal that alanine can recognize the target metal ions with no significant deviation in their signals in the presence of the 2 mM concentrations of added interfering ions such as K^+, Na^+, As^{3+}, Ag^+, Cs^+, Ca^{2+}, Sr^{2+}, Co^{2+}, Pb^{2+}, and Cl^- and surfactants, complexing agents, and organic compounds like SDS, CTAB, EDTA, citric acid, glucose, 2-amino-4-nitrophenol, and 3-chloro-5-nitrophenol. Hence, Figure 7A confirms the selectivity and absolute discrimination ability of our sensor to extract Cd^{2+}, Cu^{2+}, Zn^{2+}, and Hg^{2+} ions simultaneously in the presence of multifold concentrations of interfering species attributed to strong metal ion affinity for the modifier at the GCE. The oxidative stripping peak current variations with and without interfering species are presented as a bar graph in Figure 7B and do not show any significant effect on the SWASV current signals for the targeted metal ions.

The stability and reliability of the designed electrode, that is, test−retest consistency of a sensor, were assessed by recording successive four SWASVs at a single-modified electrode for 10 μM Zn^{2+}, 7.5 μM Cd^{2+}, 5 μM Cu^{2+}, and 7.5 μM Hg^{2+} ions detection in BRB (pH 4) under predetermined optimum conditions, and their voltammograms displayed no significant variation in electrochemical responses on repetitive measurements as revealed in Figure 8A. The relative standard deviation (RSD) values of an alanine-immobilized electrode were found to be below 2% that represents excellent repeatability, stability, and durability of the electrode. In a similar fashion, four different GC electrodes were modified by alanine to check precise reproducibilities of the fabricated electrodes. All electrodes displayed almost identical voltammetric signals with relative standard deviation (RSD) values below 5% as shown in Figure 8B. Measured figure of merits of the designed sensor are summarized in Table 3. This showed that our proposed sensor is highly stable and durable due to its great repeatability and reproducibility.

2.4. Application of the Designed Sensor to Real Water Samples. The accuracy, applicability, and validity of the proposed methodology for sensing of multiple water toxins were investigated by using tap water and drinking water samples collected from different sources in Islamabad, Pakistan. The samples were filtered to remove residues and solid impurities and diluted by adding pH 4 BRB in the 1:1 ratio, and then, recovery tests were applied by spiking known amounts of metal ions in samples to check precision and validity of the fabricated electrode under optimum conditions. Quantities of metal ions in the real samples were then evaluated by comparing their peak current values with the calibration plots. In Table 4, percentage age recoveries for our studied metal ions lies in the range from 90.2 to 99.6% with RSD values less than 3.6%, which demonstrates robustness and selectively of the developed sensor in detecting multiple metal ions with naturally occurring interfering species in real water samples. This ensures feasibility and precision of the designed sensor.

2.5. Theoretical Calculation for Designed AA/GCE Sensor. The experimental findings were verified by theoretical binding parameters of tested amino acid sensors by computational calculations using Hyper Chem 8.0 software. First, the molecular geometry of tested amino acid molecules was optimized by applying a semiempirical AM1 method on their structure. Then, by computing single point energy, functional parameters like the highest occupied and lowest unoccupied molecular orbital energies, binding energies, and heat of formation were determined to calculate chemical descriptors such as the band gap energy, ionization energy, electrophilicity index, electron affinity, electronegativity, chemical hardness, global softness, and chemical potential values[52] as summarized in Table 5. The pictorial representation of frontier molecular orbitals such as HOMO of tested amino acids is presented in

DOI: 10.1021/acsomega.9b03189
ACS Omega 2019, 4, 22057−22068

Table 2. Comparison of some Figures of Merit Related to the Different Reported Modified Electrodes for the Sensing Ability of Zn^{2+}, Cd^{2+}, Cu^{2+} and Hg^{2+} Ions[a]

sensors	measurement technique	LOD (nM)				ref
		Zn^{2+}	Cd^{2+}	Cu^{2+}	Hg^{2+}	
Cu-CoHCF/GCE with L-cysteine	DPV	N.M	N.M	N.M	80	9
DAN/GCE	SWASV	N.M	N.M	N.M	640	10
Ag NPs	Optical	N.M.	N.M.	500	N.M.	26
GO/GCE with poly L-glutamic acid	DPASV	N.M.	15	24	32	32
N-G/GCE	DPSV	N.M*	50	5	50	33
CNT threads	SWASV	1.40	1.90	0.27	N.M.	34
Pd/PAC-GCE	DPV	N.M.	41	66	54	35
GC−IIP−MWCNTs	DPASV	N.M.	N.M.	N.M	5	37
BiONPs-CS/GCE	DPASV	N.M.	50	N.M	N.M.	38
AuNPs/GCE	DPSV	N.M.	N.M.	N.M	1000	39
SNAC/GCE	DPV	N.M.	24.4	23.2	24.6	40
IL/SBA 15-silica/CPE	DPASV	N.M	80	60	10	41
chitosan/GCE	DPASV	N.M.	667	2350	N.M.	42
CdTe QDs	PL	500	120	N.M	N.M.	43
G-MWCNTs	DPASV	N.M	100	N.M	N.M	44
GCE/MMT/TBAB (partial)/M		N.M	72	36	N.M	45
WBMCPE NCFs-MCPE		N.M	N.M	N.M	147.6	46
dithizone-PVC membrane/Ag electrode	CV	N.M.	N.M.	830	N.M.	47
SnO_2/RGO nanocomposite	SWASV	N.M	0.1	0.23	0.28	48
cysteine/CPG	AAS	0.2	0.1	0.1	30	49
RGO-CS/GCE with poly L-Lysine	DPASV	N.M	10	20	N.M	50
Ala/GCE	SWASV	8.9×10^{-3}	5.8×10^{-3}	3.0×10^{-3}	5.9×10^{-3}	this work

[a]CPE: carbon paste electrode; BiONPs-CS: bismuth oxide nanoparticles-chitosan; AuNPs: gold nanoparticles; SNAC: spherical carbon nanoparticle-decorated activated carbon; Cu-CoHCF: copper-cobalt hexacyanoferrate; GCE: glassy carbon electrode; AgNPs: silver nanoparticles; CNT: carbon nanotube; TBAB: tetrabutylammonium-modified clay film electrodes; SBA 15-silica: silica organofunctionalized with 2-benzothiazolethiol; Pd/PAC: palladium nanoparticles on porous activated carbons; PGA/GO: poly(L-glutamic acid) (PGA) and graphene oxide (GO) composite; DAN: 1-(2,4-dinitrophenyl)-dodecanoylthiourea; WBMCPE: water hyacinth biomass-modified carbon paste electrodes; RGO-CS: reduced graphene oxide-chitosan; CdTe QDs: cadmium telluride quantum dots; PL: photoluminescence; Ala = L-alanine; *N.M. = not measured.

Figure 9. Chemical activity of modifiers and the extent of favorable interactions between amino acid molecules and metal ions can be assessed by energy band gap values. The band gap energy of alanine (−11.26 eV) is much higher compared to band gap energies of threonine, glutamic acid, and lysine (−11.11, −11.20, and −10.62 eV, respectively), which strongly suggest alanine's high affinity for metal ions coordination. Similarly, high chemical hardness and low global softness values of alanine as compared to other amino acids used as recognition layers corresponds to a larger frontier orbital gap that leads to a kinetically more stable molecular structure. Moreover, the alanine amino acid was observed to show the lowest binding energy (−1214.25 kcal/mol), that is, more stability than threonine, glutamic acid, and lysine amino acids, which supports our experimental findings that alanine can develop more effective interactions with targeted metal ions than other tested amino acids and can be used as the best metal ion sensor amongst them.

The complexation mechanism due to effective interactions between alanine and targeted metal ions was further explored by computational modeling with computational density functional (DFT) program with a B3LYP/LANL2DZ basis set at Gaussview 5.0 software. The chemical descriptors were analyzed from HOMO and LUMO energy values of optimized molecular geometries of alanine and its metal complexes as listed in Table 6. Comparison of metal−alanine complexes with individual entities reveals that complexes have a low value of the frontier orbital gap and chemical hardness, consequently high global softness, more polarizable structure, and high electrophilicity index that relates to high chemical reactivity and instability is observed. Theoretically, the total energy value appears more negative for the alanine−copper ion complex Cu^{2+}−Ala (−518.62 hartree) than the rest of alanine−metal ion complexes Zn^{2+}−Ala, Hg^{2+}−Ala, and Cd^{2+}−Ala (−388.70, −365.83, and −371.16 hartree, respectively) suggestive of strong complexation of the copper ion with alanine compared to other metal ions present in solution. However, total energy values for all complexes are more negative in contrast to free alanine (−323.70 hartree) that support an effective interaction between the alanine recognition layer and analytes. The complexation and decomplexation of metals ions occur during reductive deposition and oxidative stripping steps of SWASV. Hence, these theoretical studies not only support the experimental findings but also offer a working mechanism of the sensor suggesting how alanine acts as a mediator to facilitate charge transduction between the guest (metal ions) and the host (electrode) via the complexation process.

3. CONCLUSIONS

An efficient transducer based on L-alanine amino acid as a recognition layer was developed for sequestering the multiple water toxins (Zn^{2+}, Cd^{2+}, Cu^{2+}, and Hg^{2+} ions) that exist in aqueous bodies. EIS, CV, and SWASV results not only ensured fabrication and robustness of charge transfer at the interfacial electrode surface but also verified significantly boosted current signals for detection of multitarget analytes at alanine-

DOI: 10.1021/acsomega.9b03189
ACS Omega 2019, 4, 22057−22068

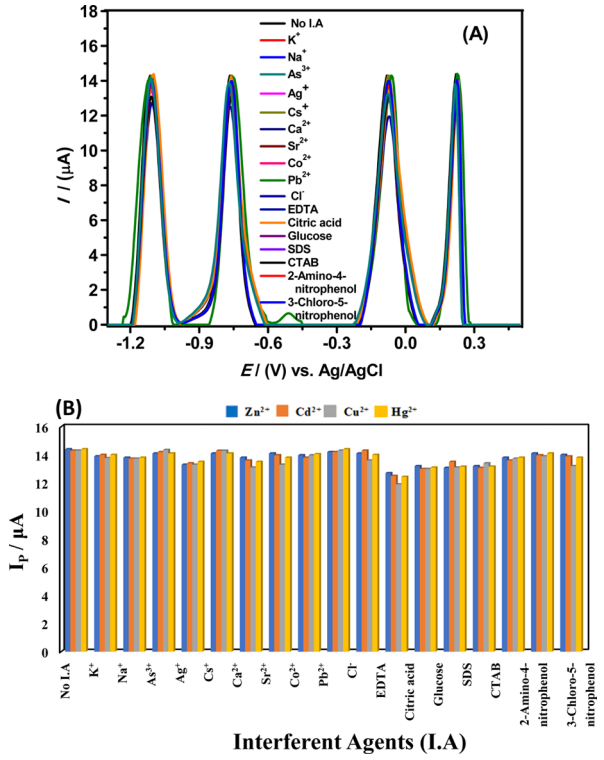

Figure 7. (A) Voltammograms of metal analytes performed with an alanine-modified electrode in the presence of 2 mM of one of the interfering agents, i.e., K^+, Na^+, As^{3+}, Ag^+, Cs^+, Ca^{2+}, Sr^{2+}, Co^{2+}, Pb^{2+}, Cl^-, EDTA, citric acid, glucose, SDS, CTAB, 2-amino-4- nitrophenol, and 3-chloro-5-nitrophenol in cell having 10 μM Zn^{2+}, 7.5 μM Cd^{2+}, 5 μM Cu^{2+}, and 7.5 μM Hg^{2+} ions in BRB of pH 4 under chosen optimized conditions. (B) Corresponding bar graphs showing adsorptive stripping peak current I_p of SWASV affected by 2 mM concentrations of various ions and organic interfering agents.

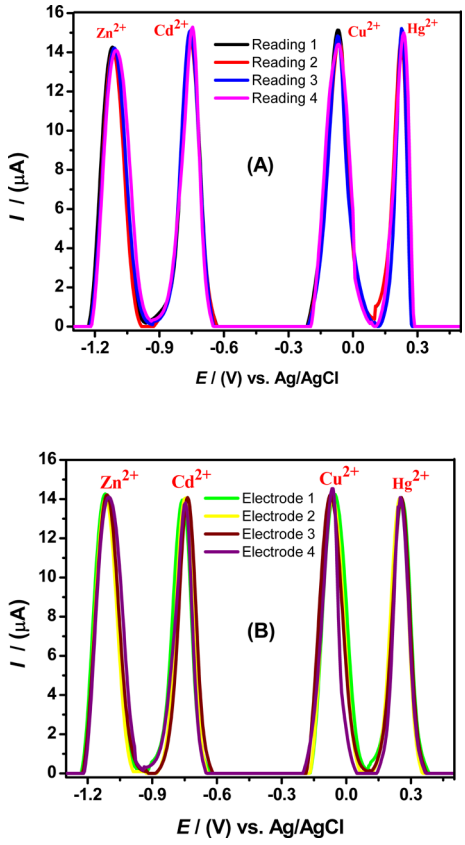

Figure 8. Validation of the applied methodology by monitoring the SWASV peak current responses of 10 μM Zn^{2+}, 7.5 μM Cd^{2+}, 5 μM Cu^{2+}, and 7.5 μM Hg^{2+} ion solutions under chosen optimized conditions; (A) showing repeatability of the designed Ala/GCE electrode at multiple scans (n = 4) and (B) SWASV showing reproducibility of multiple fabricated Ala/GCE electrodes (n = 4)

immobilized GCE compared to bare GCE. Furthermore, SWASV sensing conditions, that is, modifier concentrations, stripping electrolytes, pH of solution, deposition potentials, and accumulation time for preconcentrations of metal ions, were optimized to achieve the maximum current signals by effective coordination of L-alanine with targeted analytes. The alanine recognition layer demonstrated absolute discrimination ability and selectivity in the presence of multifold interferents, remarkable electrocatalytic activity, reproducibility, stability, and extraordinary sensitivity for metal-based water toxins even under harsh conditions such as the presence of multifold interferents. Moreover, the linear concentration range for the designed multitargeted metal sensors lead to determine ultratrace picomolar LOD and LOQ values that are far lower than threshold contamination levels of Zn^{2+}, Cd^{2+}, Cu^{2+}, and Hg^{2+} ions suggested by EPA and WHO for drinking water. Additionally, computational studies support experimental parameters, and the novel role of alanine as a mediator for charge transfer between the recognition layer and analytes by the mechanism of complexation−decomplexation is ascertained. Moreover, the designed sensing platform demonstrates excellent figures of merit in the context of percentage age recoveries of real samples, hence offers its applicability as a promising analytical tool.

4. EXPERIMENTAL SECTION

4.1. Chemicals. Chemicals used in present work are L-alanine, L-lysine, L-threonine, L-glutamic acid, zinc acetate, cadmium chloride, cupric chloride, mercuric chloride, acetic acid, HCl, NaOH, KCl, H_2SO_4, H_3BO_3, H_3PO_4, acetonitrile CAN, NBu_4BF_4, sodium acetate, sodium phosphate dibasic heptahydrate, arsenic chloride, silver chloride, strontium nitrate, cesium chloride, chromium chloride, sodium chloride, cobalt chloride, lead nitrate, sodium phosphate monobasic monohydrate, calcium chloride, surfactants (CTAB, SDS), EDTA, glucose, citric acid, 2-amino-4-nitrophenol, and 3-chloro-5-nitrophenol. All chemicals selected as analytes, recognition layers, electrolytes, and interfering agents were procured from Sigma-Aldrich and utilized as received. All solutions were prepared in doubly distilled water. Moreover, to investigate the validity of the designed sensor in real water system, tap, and drinking water samples were collected from different sources in Islamabad, Pakistan.

4.2. Instrumentation. For electrochemical investigation, cyclic voltammetry (CV), electrochemical impedance spectroscopy (EIS), and square-wave anodic stripping voltammetry (SWASV) were performed on a Metrohm Auto lab PGSTAT302N having FRA and NOVA 1.11 software. A typical three-electrode system was used that consists of a Pt wire as the counter electrode, a reference electrode constituting the Ag/AgCl (3 M KCl) electrode, and a bare glassy carbon electrode (GCE) or an amino acid-modified

DOI: 10.1021/acsomega.9b03189
ACS Omega 2019, 4, 22057−22068

Table 3. Figures of Merits for the Alanine Modified GCE

metal ions	investigated range (μM−nM)	linearity range (μM−nM)	LOD (pM)	LOQ (pM)	%RSD (reproducibility) (n = 4)	%RSD (repeatability) (n = 4)
Zn^{2+}	100−10	10−10	8.92	30.0	3.83	0.64
Cd^{2+}	75−7.5	7.5−7.5	5.77	19.0	2.05	1.52
Cu^{2+}	50−5	5−5	3.01	10.0	3.92	1.58
Hg^{2+}	75−7.5	7.5−7.5	5.89	20.0	1.73	1.22

Table 4. Results for Zn^{2+}, Cd^{2+}, Cu^{2+}, and Hg^{2+} Determination in Real Water Samples Obtained under the Optimum Experimental Conditions

metal ions	sample	initially found (μM)	spiked amount (μM)	found (μM)	RSD (%)	recovery (%)
Zn^{2+}	drinking water 1	0.00	10.0	9.90	1.25	99.0
	drinking water 2	0.00	10.0	9.74	1.82	97.4
	tap water 1	0.00	10.0	9.50	2.50	95.0
	tap water 2	0.00	10.0	9.68	1.90	96.8
Cd^{2+}	drinking water 1	0.00	7.5	7.23	1.96	96.4
	drinking water 2	0.00	7.5	7.45	3.02	99.6
	tap water 1	0.00	7.5	7.43	1.87	99.0
	tap water 2	0.00	7.5	7.22	1.11	96.4
Cu^{2+}	drinking water 1	0.00	5.0	4.86	1.90	97.2
	drinking water 2	0.00	5.0	4.77	2.63	95.4
	tap water 1	0.00	5.0	4.58	1.84	91.6
	tap water 2	0.00	5.0	4.51	3.58	90.2
Hg^{2+}	drinking water 1	0.00	7.5	7.39	2.90	98.5
	drinking water 2	0.00	7.5	7.12	0.95	94.9
	tap water 1	0.00	7.5	6.96	1.70	93.0
	tap water 2	0.00	7.5	7.3	2.70	97.0

Table 5. Comparative Data Showing Chemical Reactivity Descriptors of Alanine, Threonine, Glutamic Acid, and Lysine Amino Acids

structural parameters	alanine	threonine	glutamic acid	lysine
total energy (kcal/mol)	−30659.19	−41644.40	−51997.75	−46530.97
heat of formation (kcal/mol)	−104.75	−153.99	−201.17	−120.39
binding energy (kcal/mol)	−1214.25	−1598.14	−1875.77	−2220.27
E_{HOMO} (eV)	−10.32	−10.21	−10.53	−9.74
E_{LUMO} (eV)	0.94	0.91	0.67	0.91
ionization energy [IE $(-\varepsilon_{HOMO})$]	10.32	10.21	10.53	9.74
electron affinity [EA $(-\varepsilon_{LUMO})$]	1-0.94	−0.91	−0.67	−0.91
band gap (eV) $[E_{HOMO} - E_{LUMO}]$	−11.26	−11.11	−11.20	−10.65
electronegativity (eV) χ [(IE + EA)/2	4.69	4.65	4.93	4.41
chemical potential μ $(-\chi)$	−4.69	−4.65	−4.93	−4.41
chemical hardness (eV) η [(IE− EA)/2]	5.63	5.55	5.6	5.31
chemical Softness (eV) σ $(1/\eta)$	0.177	0.180	0.178	0.188
electrophilicity Index Ω $(\mu^2/2\eta)$	1.95	1.94	2.17	1.83

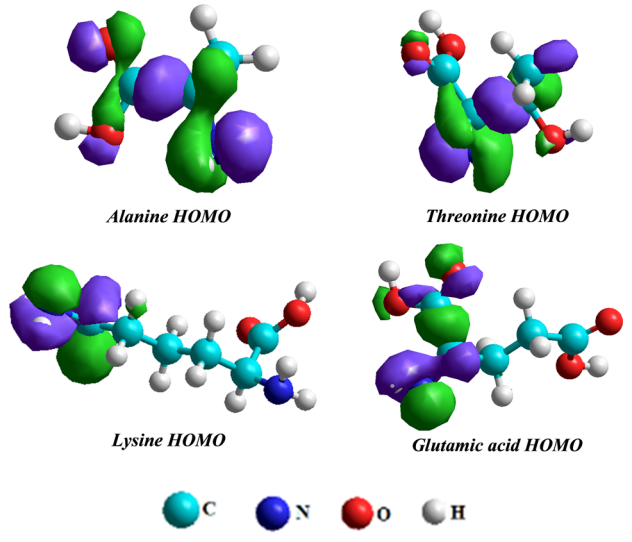

Figure 9. Pictorial representation of HOMO (the highest occupied molecular orbital) of optimized structures of alanine, threonine, glutamic acid, and lysine amino acids by Hyperchem 8.0 software using semiempirical AM1 method.

glassy carbon electrode (AA/GCE) as the working electrode. The working electrode was positioned at the least distance from the reference electrode to minimize the IR drop effect. The pH values of all electrolytes and solutions were adjusted by using a 620 lab pH meter. All analytical data was collected at room temperature. An inert atmosphere was maintained above analytical solutions through continuous nitrogen gas purging.

4.3. Methodology for Electrode Modification. For electrode fabrication, a bare glassy carbon electrode was gently rub on 6 and 1 μm alumina slurries having a nylon buffing pad repeatedly to achieve a smooth shiny surface. Then, the polished electrode was thoroughly washed with doubly distilled water. To obtain reproducible surface conditions before modification, physical pretreatment was followed by electro-

DOI: 10.1021/acsomega.9b03189
ACS Omega 2019, 4, 22057−22068

Table 6. Comparative Data Showing Chemical Reactivity Descriptors (in Terms of Hartree Units) of Alanine and Alanine−Metal Complexes

structural parameters	αlanine	Cu^{2+}−Ala	Zn^{2+}−Ala	Hg^{2+}−Ala	Cd^{2+}−Ala
total energy (E)	−323.70	−518.62	−388.70	−365.83	−371.16
E_{HOMO}	−0.56	−0.212	−0.195	−0.220	−0.201
E_{LUMO}	−0.004	−0.094	−.031	−0.033	−0.040
ΔE gap [$E_{HOMO} - E_{LUMO}$]	0.252	0.119	0.164	0.187	0.162
ionization energy IE ($-\varepsilon_{HOMO}$)	0.256	0.212	0.195	0.220	0.201
electron affinity EA ($-\varepsilon_{LUMO}$)	0.004	0.094	0.031	0.033	0.040
electronegativity χ [(IE + EA)/2]	0.13	0.15	0.11	0.12	0.12
chemical potential μ ($-\chi$)	−0.13	−0.15	−0.11	−0.12	−0.12
chemical hardness η [(IE− EA)/2]	0.126	0.060	0.082	0.094	0.081
chemical softness σ ($1/\eta$)	7.94	16.80	12.17	10.70	12.30
electrophilicity index Ω ($\mu^2/2\eta$)	0.067	0.19	0.073	0.076	0.088

chemical pretreatment by passing the electrode surface through several polarization cycles of −1.4 to +0.9 V in buffer media at 100 mVs^{-1} until reproducible cyclic voltammogram was accomplished.

Then, the clean activated electrode surface was covalently modified via electrochemical-aided grafting of the known concentration of amino acids on the carbon surface. To obtain modified electrode having a stable monolayer with a broad potential range, bare GCE was scanned four times between 0 to +1.4 V with a scan rate of 10 mV/s by a cyclic voltammetric technique in the solution of the selected amino acid in acetonitrile (ACN) having 0.1 M NBu_4BF_4 under inert atmosphere. At a sufficiently positive potential, controlled electrolysis of amino acid solution causes electrooxidation of its amino group and produces a corresponding cation radical that forms carbon−nitrogen covalent linkage at the electrode surface. Thus, individual amino acids are grafted onto GCE through its N-terminus and allow the binding of analytes from their carboxylic acid terminus during the complexation process as shown in the modification Scheme 1.[25,53] The modified

Scheme 1. Grafting of Amino Acids on GCE Surface

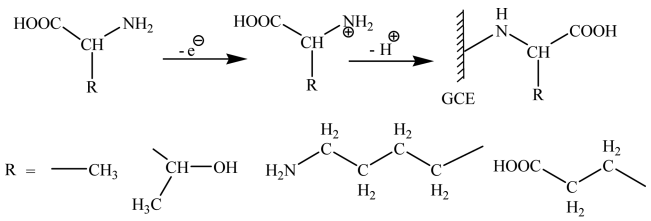

R=Side chains of Alanine, threonine, lysine and glutamic acid

electrode was cautiously cleaned with ethanol and doubly distilled water to remove any physiosorbed, unreacted, and loosely bound amino acid molecules. All cyclic voltammograms with AA/GCE as WE in 0.1 M KCl in a potential range between −1.5 to +0.8 V, that is, working potential window for metal ions, revealed no redox peak for amino acids. The prepared AA/modified electrodes are ready to be used and can be stored in PBS (phosphate buffer) of pH 6.0 at 4 °C.[54,55] For simultaneous detection of toxic metal ions, the modified electrode was then subjected to square-wave anodic stripping voltammetry (SWASV), which involves a deposition step where a predefined deposition potential of −1.3 V for a 140 s deposition time is applied to electroplate metal ions on the electrode surface. While in the stripping step, the electro-reduced metal ions are oxidized back into the solution during anodic stripping with a potential scan ranging from −1.3 to 0.8 V.

AUTHOR INFORMATION

Corresponding Author

*E-mail: Dr. Afzal Shah afzals_qau@yahoo.com.

ORCID

Faiza Jan Iftikhar: 0000-0002-8669-3711

Jan Nisar: 0000-0001-9291-6064

Notes

The authors declare no competing financial interest.

ACKNOWLEDGMENTS

The authors gratefully acknowledge Higher Education Commission and Quaid-i-Azam University of Pakistan for supporting this work. The authors also acknowledge the support of the University of Bahrain and the Deanship of Scientific Research (DSR), King Abdulaziz University, Jeddah, under grant No. (DF-105-130-1441).

REFERENCES

(1) Lin, W.-C.; Li, Z.; Burns, M. A. A drinking water sensor for lead and other heavy metals. *Anal. Chem.* **2017**, *89*, 8748−8756.

(2) Alias, C.; Benassi, L.; Bertazzi, L.; Sorlini, S.; Volta, M.; Gelatti, U. Environmental exposure and health effects in a highly polluted area of Northern Italy: a narrative review. *Environ. Sci. Pollut. Res.* **2019**, *26*, 4555−4569.

(3) Rodríguez, J.; Mandalunis, P. M. A Review of Metal Exposure and Its Effects on Bone Health. *J. Toxicol.* **2018**, *2018*, 4854152.

(4) Selvi, A.; Rajasekar, A.; Theerthagiri, J.; Ananthaselvam, A.; SathishKumar, K.; Madhavan, J.; Rahman, P. K. S. M. Integrated remediation processes toward heavy metal removal/recovery from various environments-a review. *Front. Environ. Sci.* **2019**, *7*, 66.

(5) Stern, B. R. Essentiality and toxicity in copper health risk assessment: overview, update and regulatory considerations. *J. Toxicol. Environ. Health, Part A* **2010**, *73*, 114−127.

(6) Plum, L. M.; Rink, L.; Haase, H. The essential toxin: impact of zinc on human health. *Int. J. Environ. Res. Public Health* **2010**, *7*, 1342−1365.

(7) Mohod, C. V.; Dhote, J. Review of heavy metals in drinking water and their effect on human health. *Int. J. Innovative Res. Sci. Eng. Technol.* **2013**, *2*, 2992−2996.

(8) Chow, E.; Hibbert, D. B.; Gooding, J. J. Voltammetric detection of cadmium ions at glutathione-modified gold electrodes. *Analyst* **2005**, *130*, 831−837.

(9) Sharma, V. V.; Tonelli, D.; Guadagnini, L.; Gazzano, M. Copper-cobalt hexacyanoferrate modified glassy carbon electrode for an indirect electrochemical determination of mercury. *Sens. Actuators, B.* **2017**, *238*, 9−15.

DOI: 10.1021/acsomega.9b03189
ACS Omega 2019, 4, 22057−22068

(10) Zahid, A.; Lashin, A.; Rana, U. A.; Al-Arifi, N.; Ullah, I.; Dionysiou, D. D.; Qureshi, R.; Waseem, A.; Kraatz, H.-B.; Shah, A. Development of surfactant based electrochemical sensor for the trace level detection of mercury. *Electrochim. Acta* **2016**, *190*, 1007−1014.
(11) Hua, C.; Zhang, W. H.; De Almeida, S. R. M.; Ciampi, S.; Gloria, D.; Liu, G.; Harper, J. B.; Gooding, J. J. A novel route to copper (II) detection using 'click' chemistry-induced aggregation of gold nanoparticles. *Analyst* **2012**, *137*, 82−86.
(12) Gumpu, M. B.; Sethuraman, S.; Krishnan, U. M.; Rayappan, J. B. B. A review on detection of heavy metal ions in water−an electrochemical approach. *Sens. Actuators, B* **2015**, *213*, 515−533.
(13) Cui, L.; Wu, J.; Ju, H. Electrochemical sensing of heavy metal ions with inorganic, organic and bio-materials. *Biosens. Bioelectron.* **2015**, *63*, 276−286.
(14) Gan, X.; Zhao, H. Understanding Signal Amplification Strategies of Nanostructured Electrochemical Sensors for Environmental Pollutants. *Curr. Opin. Electrochem.* **2019**, *17*, 56−64.
(15) Iftikhar, F. J.; Shah, A.; Akhter, M. S.; Kurbanoglu, S.; Ozkan, S. A. Introduction to Nanosensors. In *New Developments in Nanosensors for Pharmaceutical Analysis*; 1st ed.; Ozkan, S. A.; Shah, A., Eds.; Academic Press, 2019; pp 1−46.
(16) Shah, A.; Zahid, A.; Khan, A.; Iftikhar, F. J.; Nisar, J.; Fernandez, C.; Akhter, M. S.; Almutawah, A. A.; Kraatz, H. B. Development of a Highly Sensitive Electrochemical Sensing Platform for the Trace Level Detection of Lead Ions. *J. Electrochem. Soc.* **2019**, *166*, B3136−B3142.
(17) Gooding, J. J. Nanostructuring electrodes with carbon nanotubes: A review on electrochemistry and applications for sensing. *Electrochim. Acta* **2005**, *50*, 3049−3060.
(18) Aftab, S.; Ozcelikay, G.; Kurbanoglu, S.; Shah, A.; Iftikhar, F. J.; Ozkan, S. A. A novel electrochemical nanosensor based on NH_2-functionalized multi walled carbon nanotubes for the determination of catechol-orto-methyltransferase inhibitor entacapone. *J. Pharm. Biomed. Anal.* **2019**, *165*, 73−81.
(19) Zahid, A.; Shah, A.; Iftikhar, F. J.; Shah, A. H.; Qureshi, R. Surfactant modified glassy carbon electrode as an efficient sensing platform for the detection of Cd (ll) and Hg (ll). *Electrochim. Acta* **2017**, *235*, 72−78.
(20) Gooding, J.; Hibbert, D.; Yang, W. Electrochemical metal ion sensors. Exploiting amino acids and peptides as recognition elements. *Sensors* **2001**, *1*, 75−90.
(21) Chow, E.; Gooding, J. J. Peptide modified electrodes as electrochemical metal ion sensors. *Electroanalysis* **2006**, *18*, 1437−1448.
(22) Flavel, B. S.; Nambiar, M.; Shapter, J. G. Electrochemical detection of copper using a Gly-Gly-His modified carbon nanotube biosensor. *Silicon* **2011**, *3*, 163−171.
(23) Kaur, B.; Srivastava, R.; Satpati, B. Silver nanoparticle decorated polyaniline−zeolite nanocomposite material based non-enzymatic electrochemical sensor for nanomolar detection of lindane. *RSC Adv.* **2015**, *5*, 57657−57665.
(24) Zeleke, T. S.; Tsai, M.-C.; Weret, M. A.; Huang, C.-J.; Birhanu, M. K.; Liu, T.-C.; Huang, C.-P.; Soo, Y.-L.; Yang, Y.-W.; Su, W.-N.; Hwang, B. J. Immobilized Single Molecular Molybdenum Disulfide on Carbonized Polyacrylonitrile for Hydrogen Evolution Reaction. *ACS Nano* **2019**, *13*, 6720−6729.
(25) Zhang, L.; Lin, X. Covalent modification of glassy carbon electrodes with glycine for voltammetric separation of dopamine and ascorbic acid. *Fresenius' J. Anal. Chem.* **2001**, *370*, 956−962.
(26) Chen, X.; Cheng, X.; Gooding, J. J. Multifunctional modified silver nanoparticles as ion and pH sensors in aqueous solution. *Analyst* **2012**, *137*, 2338−2343.
(27) Shah, A. H.; Shah, A.; Khan, S. U. D.; Rana, U. A.; Hussain, H.; Khan, S. B.; Qureshi, R.; Badshah, A.; Waseem, A. Probing the pH dependent electrochemistry of a novel quinoxaline carboxylic acid derivative at a glassy carbon electrode. *Electrochim. Acta* **2014**, *147*, 121−128.
(28) Yang, W.; Gooding, J. J.; Hibbert, D. B. Characterisation of gold electrodes modified with self-assembled monolayers of L-cysteine for the adsorptive stripping analysis of copper. *J. Electroanal. Chem.* **2001**, *516*, 10−16.
(29) Shen, L.-L.; Zhang, G.-R.; Li, W.; Biesalski, M.; Etzold, B. J. M. Modifier-free microfluidic electrochemical sensor for heavy-metal detection. *ACS Omega* **2017**, *2*, 4593−4603.
(30) Lee, S.; Bong, S.; Ha, J.; Kwak, M.; Park, S.-K.; Piao, Y. Electrochemical deposition of bismuth on activated graphene-nafion composite for anodic stripping voltammetric determination of trace heavy metals. *Sens. Actuators, B* **2015**, *215*, 62−69.
(31) Munir, A.; Shah, A.; Nisar, J.; Ashiq, M. N.; Akhter, M. S.; Shah, A. H. Selective and simultaneous detection of Zn^{2+}, Cd^{2+}, Pb^{2+}, Cu^{2+}, Hg^{2+} and Sr^{2+} using surfactant modified electrochemical sensors. *Electrochim. Acta* **2019**, *323*, 134592.
(32) Yi, W.; He, Z.; Fei, J.; He, X. Sensitive electrochemical sensor based on poly (L-glutamic acid)/graphene oxide composite material for simultaneous detection of heavy metal ions. *RSC Adv.* **2019**, *9*, 17325−17334.
(33) Xing, H.; Xu, J.; Zhu, X.; Duan, X.; Lu, L.; Wang, W.; Zhang, Y.; Yang, T. Highly sensitive simultaneous determination of cadmium (II), lead (II), copper (II), and mercury (II) ions on N-doped graphene modified electrode. *J. Electroanal. Chem.* **2016**, *760*, 52−58.
(34) Zhao, D.; Guo, X.; Wang, T.; Alvarez, N.; Shanov, V. N.; Heineman, W. R. Simultaneous detection of heavy metals by anodic stripping voltammetry using carbon nanotube thread. *Electroanalysis* **2014**, *26*, 488−496.
(35) Veerakumar, P.; Veeramani, V.; Chen, S.-M.; Madhu, R.; Liu, S.-B. Palladium Nanoparticle Incorporated Porous Activated Carbon: Electrochemical Detection of Toxic Metal Ions. *ACS Appl. Mater. Interfaces* **2016**, *8*, 1319−1326.
(36) Jeong, E.-D.; Won, M.-S.; Shim, Y.-B. Simultaneous determination of lead, copper, and mercury at a modified carbon paste eletrode containing humic acid. *Electroanalysis* **1994**, *6*, 887−893.
(37) Rajabi, H. R.; Roushani, M.; Shamsipur, M. Development of a highly selective voltammetric sensor for nanomolar detection of mercury ions using glassy carbon electrode modified with a novel ion imprinted polymeric nanobeads and multi-wall carbon nanotubes. *J. Electroanal. Chem.* **2013**, *693*, 16−22.
(38) Hao, C.; Shen, Y.; Shen, J.; Xu, K.; Wang, X.; Zhao, Y.; Ge, C. A glassy carbon electrode modified with bismuth oxide nanoparticles and chitosan as a sensor for Pb (II) and Cd (II). *Microchim. Acta* **2016**, *183*, 1823−1830.
(39) Ratner, N.; Mandler, D. Electrochemical detection of low concentrations of mercury in water using gold nanoparticles. *Anal. Chem.* **2015**, *87*, 5148−5155.
(40) Madhu, R.; Sankar, K. V.; Chen, S.-M.; Selvan, R. K. Eco-friendly synthesis of activated carbon from dead mango leaves for the ultrahigh sensitive detection of toxic heavy metal ions and energy storage applications. *RSC Adv.* **2014**, *4*, 1225−1233.
(41) Zhang, P.; Dong, S.; Gu, G.; Huang, T. Simultaneous determination of Cd^{2+}, Pb^{2+}, Cu^{2+} and Hg^{2+} at a carbon paste electrode modified with ionic liquid-functionalized ordered mesoporous silica. *Bull. Korean Chem. Soc.* **2010**, *31*, 2949−2954.
(42) Martínez-Huitle, C.; Fernandes, N. S.; Cerro-Lopez, M.; Quiroz, M. A. Determination of trace metals by differential pulse voltammetry at chitosan modified electrodes. *Port. Electrochim. Acta* **2010**, *28*, 39−49.
(43) Xu, H.; Miao, R.; Fang, Z.; Zhong, X. Quantum dot-based "turn-on" fluorescent probe for detection of zinc and cadmium ions in aqueous media. *Anal. Chim. Acta* **2011**, *687*, 82−88.
(44) Huang, H.; Chen, T.; Liu, X.; Ma, H. Ultrasensitive and simultaneous detection of heavy metal ions based on three-dimensional graphene-carbon nanotubes hybrid electrode materials. *Anal. Chim. Acta* **2014**, *852*, 45−54.
(45) Maghear, A.; Tertiş, M.; Fritea, L.; Marian, I. O.; Indrea, E.; Walcarius, A.; Săndulescu, R. Tetrabutylammonium-modified clay film electrodes: Characterization and application to the detection of metal ions. *Talanta* **2014**, *125*, 36−44.

DOI: 10.1021/acsomega.9b03189
ACS Omega 2019, 4, 22057−22068

(46) Bahrami, A.; Besharati-Seidani, A.; Abbaspour, A.; Shamsipur, M. A highly selective voltammetric sensor for nanomolar detection of mercury ions using a carbon ionic liquid paste electrode impregnated with novel ion imprinted polymeric nanobeads. *Mater. Sci. Eng. C* **2015**, *48*, 205−212.
(47) Othman, M. A. F.; Othman, A. A.; Zuki, H. M. Dithizone modified silver electrode for the determination of metal ions in aqueous solution. *MJAS* **2016**, *20*, 197−204.
(48) Wei, Y.; Gao, C.; Meng, F.-L.; Li, H.-H.; Wang, L.; Liu, J.-H.; Huang, X.-J. SnO_2/reduced graphene oxide nanocomposite for the simultaneous electrochemical detection of cadmium (II), lead (II), copper (II), and mercury (II): an interesting favorable mutual interference. *J. Phys. Chem. C* **2012**, *116*, 1034−1041.
(49) Elmahadi, H. A. M.; Greenway, G. M. Immobilized cysteine as a reagent for preconcentration of trace metals prior to determination by atomic absorption spectrometry. *J. Anal. At. Spectrom.* **1993**, *8*, 1011−1014.
(50) Guo, Z.; Li, D.-d.; Luo, X.-k.; Li, Y.-h.; Zhao, Q.-N.; Li, M.-m.; Zhao, Y.-t.; Sun, T.-s.; Ma, C. Simultaneous determination of trace Cd (II), Pb (II) and Cu (II) by differential pulse anodic stripping voltammetry using a reduced graphene oxide-chitosan/poly-l-lysine nanocomposite modified glassy carbon electrode. *J. Colloid Interface Sci.* **2017**, *490*, 11−22.
(51) Abu-Dalo, M. A.; Salam, A. A.; Nassory, N. S. Ion imprinted polymer based electrochemical sensor for environmental monitoring of copper (II). *Int. J. Electrochem. Sci.* **2015**, *10*, 6780−6793.
(52) Esmaielzadeh, S.; Mashhadiagha, G. Formation constants and thermodynamic parameters of bivalent Co, Ni, Cu and Zn complexes with Schiff base ligand: Experimental and DFT calculations. *Bull. Chem. Soc. Ethiop.* **2017**, *31*, 159−170.
(53) Downard, A. J. Electrochemically assisted covalent modification of carbon electrodes. *Electroanalysis* **2000**, *12*, 1085−1096.
(54) Zhang, L.; Lin, X. Electrochemical behavior of a covalently modified glassy carbon electrode with aspartic acid and its use for voltammetric differentiation of dopamine and ascorbic acid. *Anal. Bioanal. Chem.* **2005**, *382*, 1669−1677.
(55) Zhang, L.; Lin, X. Covalent modification of glassy carbon electrode with glutamic acid for simultaneous determination of uric acid and ascorbic acid. *Analyst* **2001**, *126*, 367−370.

DOI: 10.1021/acsomega.9b03189
ACS Omega 2019, 4, 22057−22068